



HAL
open science

Is There a Representative Elementary Volume for Anomalous Dispersion?

Alexandre Puyguiraud, Philippe Gouze, Marco Dentz

► **To cite this version:**

Alexandre Puyguiraud, Philippe Gouze, Marco Dentz. Is There a Representative Elementary Volume for Anomalous Dispersion?. *Transport in Porous Media*, 2020, 131 (2), pp.767-778. 10.1007/s11242-019-01366-z . hal-03092698

HAL Id: hal-03092698

<https://hal.science/hal-03092698>

Submitted on 2 Jan 2021

HAL is a multi-disciplinary open access archive for the deposit and dissemination of scientific research documents, whether they are published or not. The documents may come from teaching and research institutions in France or abroad, or from public or private research centers.

L'archive ouverte pluridisciplinaire **HAL**, est destinée au dépôt et à la diffusion de documents scientifiques de niveau recherche, publiés ou non, émanant des établissements d'enseignement et de recherche français ou étrangers, des laboratoires publics ou privés.

1 **Is there a representative elementary volume for anomalous**
2 **dispersion?**

3 **Alexandre Puyguiraud, Philippe Gouze and**
4 **Marco Dentz**

5
6 Received: date / Accepted: date

7 **Abstract** The concept of the representative elementary volume (REV) is often as-
8 sociated with the notion of hydrodynamic dispersion and Fickian transport. How-
9 ever, it has been frequently observed experimentally and in numerical pore scale
10 simulations that transport is non-Fickian and cannot be characterized by hydrody-
11 namic dispersion. Does this mean that the concept of the REV is invalid? We investi-
12 gate this question by a comparative analysis of the advective mechanisms of Fickian
13 and non-Fickian dispersion and their representation in large scale transport models.
14 Specifically, we focus on the microscopic foundations for the modeling of pore scale
15 fluctuations of Lagrangian velocity in terms of Brownian dynamics (hydrodynamic
16 dispersion) and in terms of continuous time random walks, which account for non-
17 Fickian transport through broad distributions of advection times. We find that both
18 approaches require the existence of an REV that, however, is defined in terms of the
19 representativeness of Eulerian flow properties. This is in contrast to classical defini-
20 tions in terms of medium properties such as porosity, for example.

21 **Keywords** Representative elementary volume · upscaling · anomalous dispersion ·
22 continuous time random walks · velocity statistics

A. Puyguiraud
Spanish National Research Council (IDAEA-CSIC), 08034 Barcelona, Spain
Géosciences Montpellier, CNRS-Université de Montpellier, Montpellier, France
E-mail: alexandre.puyguiraud@cid.csic.es

P. Gouze
Géosciences Montpellier, CNRS-Université de Montpellier, Montpellier, France
E-mail: philippe.gouze@univ-montp2.fr

M. Dentz
Spanish National Research Council (IDAEA-CSIC), 08034 Barcelona, Spain
E-mail: marco.dentz@csic.es

1 Introduction

The notion of a representative elementary volume (REV) lies at the heart of macroscopic (continuum) descriptions for systems that exhibit small scale structural disorder (caused by the mixture of void and solid phases that forms the porous medium), feature which is usually referred to as material heterogeneity. In the frame of continuum approaches, the REV is associated to a point of the continuous field where average properties, that are supposed to denote the effective properties of the material, are allocated. For instance permeability, from which the average fluid velocity is derived, and hydrodynamic dispersion are critical properties for modeling steady state flow and solute transport, respectively. The REV corresponds to the (minimum) volume required to evaluate the effective properties of a heterogeneous material or, in other words, the minimum volume above which the properties are stationary. This is illustrated in Figure 1 for the ratio of void to bulk volume, i.e. the porosity, where the REV size is determined from the constant limit value of ϕ_ℓ :

$$\phi_\ell = \frac{1}{V_\ell} \int_{\Omega_\ell} d\mathbf{x} \mathbb{I}(\mathbf{x} \in \Omega_f), \quad (1)$$

where Ω_f and Ω_ℓ denote the fluid domain and bulk domain of volume ℓ , V_ℓ respectively and $\mathbb{I}(\cdot)$ is the indicator function, which is equal to 1 if its argument is true and 0 otherwise. The length scale ℓ at which ϕ_ℓ stabilizes defines the REV scale.

Accordingly, the REV is clearly definable for two extreme cases: 1) unit volume in a periodic microstructure, and 2) a volume containing a large set of micro-scale structures displaying homogeneous and ergodic properties. The existence of the REV relies on the existence of scale separation of spatial medium fluctuations. An REV cannot be defined for continuously hierarchized heterogeneous media such as fractal materials. The REV is typically determined from applying this concept to the material microstructure and specifically to its simplest quantitative notion, which is its porosity (as illustrated in Figure 1). Porosity is easily measurable at laboratory scale and can also be determined at pore-scale by using imaging methods such as computed microtomography which allows characterizing the micro-structures over volumes that are typically larger than the REV. Since the REV can be well-defined for porosity, it is generally assumed that this definition also implies the existence of transport relevant parameters such as the specific discharge and the hydrodynamics dispersion coefficients. The former represents the mean pore velocity, the latter quantifies its fluctuations. The values of these parameters are considered to be well-defined and constant on the REV scale. Note that assuming the specific discharge constant within the REV implies that the product of permeability and the pressure gradient is constant. This stems from the Darcy equation, which states that

$$q = -\frac{k}{\mu} \frac{dP(x_1)}{dx_1}, \quad (2)$$

where k is permeability, $P(x_1)$ is pressure and μ dynamic viscosity. The assumption that the REV for the porosity and the specific discharge are the same is not evident. The assumption that the REV for the porosity and for the hydrodynamics dispersion

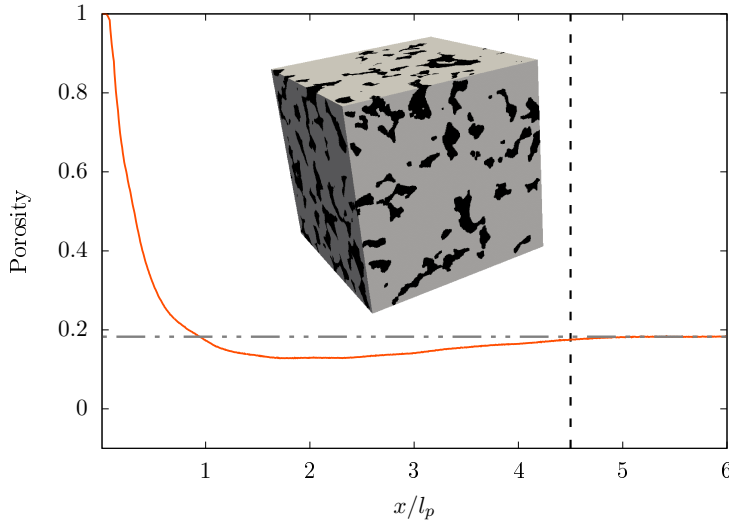


Fig. 1 Porosity measured in a cube of increasing side length cube (x -axis) centered in the middle of the Berea sandstone sample studied in Section 2. The side length of the full sample is $6\ell_p$ and its porosity is 0.182 (gray dashed line). $\ell_p \approx 1,5 \cdot 10^{-4}$ m denotes the average pore length.

65 coefficients are similar is even less evident because the later encompasses the im-
 66 pact of pore-scale velocity fluctuations. Yet, if this assumption holds, average solute
 67 transport can be described by the advection-dispersion equation (ADE) (Bear, 1972)

$$68 \quad \phi \frac{\partial c(x_1, t)}{\partial t} + q \frac{\partial c(x_1, t)}{\partial x_1} - \mathcal{D} \frac{\partial^2 c(x_1, t)}{\partial x_1^2} = 0. \quad (3)$$

69

70 This approach described Darcy-scale transport in terms of porosity ϕ , specific dis-
 71 charge q and the hydrodynamic dispersion coefficient \mathcal{D} .

72 Experimental (Moroni and Cushman, 2001; Cortis and Berkowitz, 2004; Holzner
 73 et al, 2015; Morales et al, 2017) and numerical (Bijeljic and Blunt, 2006a; Bijeljic
 74 et al, 2011; Liu and Kitanidis, 2012; De Anna et al, 2013; Kang et al, 2014; Meyer
 75 and Bijeljic, 2016; Puyguiraud et al, 2019a; Dentz et al, 2018) pore scale studies
 76 observed deviations from predictions based on the ADE (3). This includes tailing in
 77 solute breakthrough curves, non-linear growth of dispersion and non-Gaussian par-
 78 ticle distributions and propagators. Such behaviors are usually modeled based on
 79 non-local transport approaches such as multirate mass transfer and continuous time
 80 random walks (Berkowitz et al, 2006; Noetinger et al, 2016) as well as fractional
 81 dynamics (Cushman and Moroni, 2001).

82 In this paper, we investigate the notion of REV for non-Fickian dispersion. We
 83 scrutinize the assumptions underlying modeling approaches for Fickian and non-
 84 Fickian dispersion and the relation with the REV concept. In Section 2.2.1 we discuss
 85 the bases of the ADE framework and we include a critical revision of its limitations.
 86 In Section 2.2.2 we discuss the framework of continuous time random walk models

87 and investigate what underlying assumptions they are relying on. This leads us to
 88 define, in Section 2.3 the Eulerian REV for anomalous transport and to illustrate its
 89 evaluation from computations performed using a digitized volume of a real rock sam-
 90 ple in Section 2.5. The implications of such an REV definition for continuum scale
 91 modeling of Fickian and non-Fickian transport are discussed in section 3.

92 **2 Dispersion upscaling and the representative elementary volume**

93 In this section, we consider the assumptions that support the description of solute
 94 dispersion by advection-dispersion models and continuous time random walks. From
 95 these considerations we propose the definition of an REV in terms of the Eulerian
 96 flow statistics, and discuss conditions on the Lagrangian velocity statistics.

97 **2.1 Pore scale flow and transport**

98 Pore scale flow is described here by the Stokes equation

$$99 \quad \nabla^2 \mathbf{u}(\mathbf{x}) = -\frac{\nabla p(\mathbf{x})}{\mu}, \quad (4)$$

101 together with the incompressibility assumption $\nabla \cdot \mathbf{u}(\mathbf{x}) = 0$. The mean pressure gra-
 102 dient is aligned with the 1-direction of the coordinate system. We consider purely
 103 advective transport that is described by the kinematic equation

$$104 \quad \frac{d\mathbf{x}(t, \mathbf{a})}{dt} = \mathbf{v}(t, \mathbf{a}), \quad (5)$$

106 where $\mathbf{x}(t = 0, \mathbf{a}) = \mathbf{a}$ and $\mathbf{v}(t, \mathbf{a}) = \mathbf{u}[\mathbf{x}(t, \mathbf{a})]$ is the Lagrangian velocity. We disregard
 107 diffusion and focus on the advective particle motion along the streamlines as the sole
 108 mechanism by which the velocity field is sampled. The impact of diffusion on the
 109 results presented in the following, are discussed in Section 3. Equation (5) can be
 110 transformed into streamline coordinates $t \rightarrow s$, with

$$111 \quad \frac{ds(t)}{dt} = v(t), \quad (6)$$

113 where $v(t) = |\mathbf{v}(t)|$. This gives the equivalent system of equations

$$114 \quad \frac{d\mathbf{x}(s, \mathbf{a})}{ds} = \frac{\mathbf{v}(s, \mathbf{a})}{v(s, \mathbf{a})}, \quad \frac{dt(s, \mathbf{a})}{ds} = \frac{1}{v(s, \mathbf{a})}. \quad (7)$$

116 **2.2 Dispersion upscaling**

117 We consider the conditions under which pore-scale velocity fluctuations can be quan-
 118 tified by the concept of hydrodynamic dispersion and how this relates to the notion of
 119 an REV. Then, we discuss the same issues for continuous-time random walk models
 120 to upscale anomalous dispersion.

121 *2.2.1 Fickian dispersion*

122 In order to identify the basic assumption underlying the ADE formulation of Darcy-
 123 scale transport, we consider the Langevin equation (Gardiner, 2010) that is equivalent
 124 to the ADE (3),

$$125 \quad \frac{dx(t)}{dt} = \bar{v}_1 + v'_1(t), \quad (8)$$

127 where we decomposed the particle velocity $v_1(t)$ into its mean \bar{v}_1 and fluctuation
 128 $v'_1(t)$. The mean pore velocity is $\bar{v}_1 = q/\phi$. The velocity fluctuation $v'_1(t)$ is repre-
 129 sented by a stationary Gaussian random process characterized by 0 mean and the
 130 covariance function

$$131 \quad \langle v'_1(t)v'_1(t') \rangle = 2\mathcal{D}\delta(t-t'), \quad (9)$$

133 where \mathcal{D} is the hydrodynamic dispersion coefficient and $\delta(t)$ is the Dirac Delta. The
 134 angular brackets denote the average over the ensemble of the noise realizations. With
 135 these properties of the velocity fluctuations, Equation (8) describes Brownian dynam-
 136 ics.

137 The representation of the velocity fluctuations as a δ -correlated Gaussian pro-
 138 cess is based on several conditions. First, the velocity process needs to be stationary
 139 and ergodic. This means that its mean and variance depend only on the time lag
 140 and not on the absolute time. Second, velocity fluctuations decay exponentially fast
 141 on a characteristic correlation time scale τ_c . Furthermore, based on the assumption
 142 that the velocity distribution has finite variance, the displacement distribution, which
 143 is the sum of random velocity increments, converges towards a Gaussian distribu-
 144 tion as time increases. This is a consequence of the central limit theorem (Gardiner,
 145 2010) and warrants the modeling of the statistics of $v'_1(t)$ as Gaussian. The correla-
 146 tion model (9) is valid at observation times that are much larger than the correlation
 147 scale τ_c , which can be related to the advection time over a characteristic length scale
 148 ℓ_c ,

$$149 \quad \tau_c = \frac{\ell_c}{\bar{v}_1}. \quad (10)$$

151 This implies that for time $t \gg \tau_c$, particles must have access to the full spectrum of
 152 velocity variability. The Langevin equation (8), which is valid at $t \gg \tau_c$, thus implies
 153 that at each random walk step, particles can sample the full spectrum of random
 154 velocities. Particles become statistically equal on the time scale τ_c . This temporal
 155 notion can be related to a spatial REV scale through the length scale ℓ_c that is assumed
 156 to mark the correlation time together with the mean velocity \bar{v}_1 . Thus, the REV scale
 157 is supposed to contain a representative set of flow velocities that particles can sample
 158 with equal probability. This is discussed further in Section 2.3.

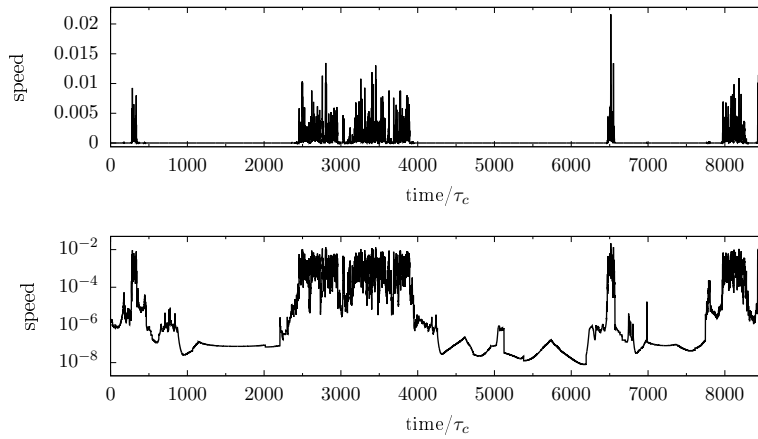


Fig. 2 Time series of velocity magnitudes experienced by a particle in the three-dimensional digitized Berea sandstone sample shown in Figure 1.

159 2.2.2 Anomalous dispersion

160 As outlined in the previous section, Brownian dynamics describes dispersion at times
 161 that are much larger than a typical correlation scale τ_c , which is equal to the transition
 162 time over an average pore length by the mean flow velocity. In order to scrutinize this
 163 condition, let us consider local transition times over the characteristic distance ℓ_c .
 164 According to (7), one can write

$$165 \quad \tau = \int_s^{s+\ell_c} \frac{ds'}{v(s')} \approx \frac{\ell_c}{v}, \quad (11)$$

166 because $v(s')$ can be considered approximately constant over a distance ℓ_c which is
 167 of the order of the pore length (Saffman, 1959). This implies that the persistence time
 168 of particles with small velocities may be much larger than suggested by τ_c . Indeed,
 169 pore-scale velocity time series have been shown to display intermittent patterns. This
 170 means that they are characterized by long periods of small velocities and rapid fluctu-
 171 ations of large amplitudes (De Anna et al, 2013; Kang et al, 2014; Morales et al,
 172 2017; Puyguiraud et al, 2019a), see also Figure 2. These patterns are indicative of
 173 a broad distribution of characteristic time scales. In fact, if the variance of τ is in-
 174 finite, a sizeable amount of particles exhibits persistence times $\tau \gg \tau_c$. This means
 175 that particles do not become statistically equal over τ_c and thus invalidates the central
 176 assumption of the Brownian dynamics approach underlying Fickian dispersion. We
 177 will show below, that this property does not invalidate the existence of an REV.

178 Particle velocities vary on spatial scales imprinted in the medium structure rather
 179 than on a fixed times scale (Kang et al, 2014; Puyguiraud et al, 2019a). This prop-
 180 erty is naturally taken into account by continuous-time random walk (CTRW) and
 181 time-domain random walk (TDRW) transport models (Berkowitz et al, 2006; Painter

182 and Cvetkovic, 2005). In the framework of these random walk approaches, the par-
 183 ticle motion along the mean flow direction is described by the following recurrence
 184 relations:

$$185 \quad x_{n+1} = x_n + \frac{\ell_c}{\chi}, \quad t_{n+1} = t_n + \tau_n, \quad (12)$$

187 where χ is the advective tortuosity (Koponen et al, 1996; Puyguiraud et al, 2019b),
 188 which measure the ratio of streamline length to average linear streamwise distance.
 189 The transition time is $\tau_n = \ell_c/v_n$. The particle velocities v_n are independent random
 190 variables. For $n = 0$, they are distributed according to an initial velocity distribution
 191 $p_0(v)$, which depends on the initial particle distribution. For $n \geq 1$, the v_n are identi-
 192 cally distributed according to the flux-weighted Eulerian velocity distribution (Dentz
 193 et al, 2016)

$$194 \quad p_s(v) = \frac{v p_e(v)}{\langle v_e \rangle}. \quad (13)$$

196 This has two consequences. First, at each random walk step particles can sample
 197 the full velocity spectrum, meaning that they are statistically equal. Second, the La-
 198 grangian velocity statistics are stationary and ergodic. Particularly, particles evolve
 199 toward their stationary steady state distribution for distances larger than the length
 200 scale ℓ_c . For these conditions to hold, it is necessary that particles can sample a rep-
 201 resentative fraction of the Eulerian velocity distribution. Thus, in the following, we
 202 define the necessary and sufficient criteria required for the existence of a velocity
 203 REV in terms of the convergence of the velocity statistics with increasing support
 204 scale. Furthermore, we discuss the issue of ergodicity and stationarity.

205 2.3 Representative elementary volume

206 As discussed in the previous section, the representativeness of the velocity statistics
 207 sampled in the support volume and the existence of a stationary velocity distribution
 208 are key properties for transport upscaling for both Fickian and non-Fickian disper-
 209 sion. Thus, the velocity statistics need to be representative of the (stationary) Eule-
 210 rian velocity statistics in the medium for the support scale to be a transport REV. We
 211 note that a volume must first be an REV for porosity because the Eulerian velocity
 212 distribution may be linked to the pore size distribution (De Anna et al, 2017; Dentz
 213 et al, 2018) and thus, evolving porosity would cause evolving velocity statistics. If the
 214 sample is an REV for porosity, then the Eulerian velocity statistics may be represen-
 215 tative. We define an REV in terms of the Eulerian velocity PDF in a similar manner as
 216 the porosity REV. A sample is considered to be a Eulerian REV if it is large enough
 217 for the Eulerian velocity distribution to become stationary. To quantify the evolution
 218 of the Eulerian velocity PDF in function of the support scale, the Eulerian velocity
 219 PDF is sampled on growing domains starting from a small volume in the center of
 220 the sample to the full sample volume. The spatially sampled PDF of the magnitude

221 of the flow velocity $v_e(\mathbf{x}) = |\mathbf{v}(\mathbf{x})|$ is defined as

$$222 \quad p_\ell(v) = \frac{1}{\phi_\ell V_\ell} \int_{\Omega_\ell} d\mathbf{x} \delta[v - v_e(\mathbf{x})] \mathbb{I}(\mathbf{x} \in \Omega_f), \quad (14)$$

223 where Ω_ℓ is the physical domain on which the PDF is computed, and V_ℓ and ϕ_ℓ are its
 224 volume and its porosity, respectively. In order to quantify accurately the convergence
 225 of these distributions toward the Eulerian PDF $p_e(v)$ for the full sample, we define
 226 the distance between $p_\ell(v)$ and $p_e(v)$ based on the Kullback-Leibler (KL) divergence
 227 (Kullback and Leibler, 1951) as

$$229 \quad d_{KL}(p_e, p_\ell) = \int_0^\infty dv p_\ell(v) \ln \left[\frac{p_\ell(v)}{p_e(v)} \right]. \quad (15)$$

230 The Kullback-Leibler divergence has been used to compare evolving PDFs to a refer-
 231 ence distribution, (see for example Bigi, 2003; Robert and Sommeria, 1991; Lindgren
 232 et al, 2004). When $d_{KL} = 0$, the distributions are identical. Here we consider a thresh-
 233 old value of $\varepsilon = 10^{-2}$ as the criterion for when the support volume can be considered
 234 an REV.

235 2.4 Lagrangian ergodicity

236 As mentioned above, the convergence of the Eulerian velocity statistics on the sup-
 237 port scale is not a sufficient condition for the upscaled random walk models to hold
 238 because these models assume by construction that particle velocities are sampled
 239 from the same stationary Lagrangian velocity PDF $p_s(v)$ at each except for the first
 240 step. In order to illustrate this, let us consider a porous media model consisting of a
 241 distribution of isolated straight capillaries. The support scale may be an REV for the
 242 Eulerian velocities. However, since the flow velocities are constant along streamlines,
 243 particles are never able to sample the full velocity spectrum.

244 The issue of Lagrangian ergodicity for pore scale flow has been studied in detail
 245 in Puyguiraud et al (2019a) in terms of the evolution of the s-Lagrangian velocity
 246 PDF, which is defined by

$$247 \quad \hat{p}_s(v, s) = \int d\mathbf{a} \rho(\mathbf{a}) \delta[v - v(s, \mathbf{a})], \quad (16)$$

248 where $\rho(\mathbf{a})$ is the initial particle distribution. We measure convergence of $\hat{p}_s(v, s)$
 249 toward the steady state $p_s(v)$ by the KL divergence $d_{KL}(\hat{p}_s, p_s)$.

251 2.5 Application to Berea sandstone sample

252 In this section we study the concept of the REV defined from the Eulerian velocity
 253 magnitude for the Berea sandstone sample illustrated in Figure 1 (Puyguiraud et al,
 254 2019a), as well as ergodicity and stationarity of the Lagrangian velocity series. The
 255 advective tortuosity of the sample is $\chi = 1.64$ (Puyguiraud et al, 2019b).

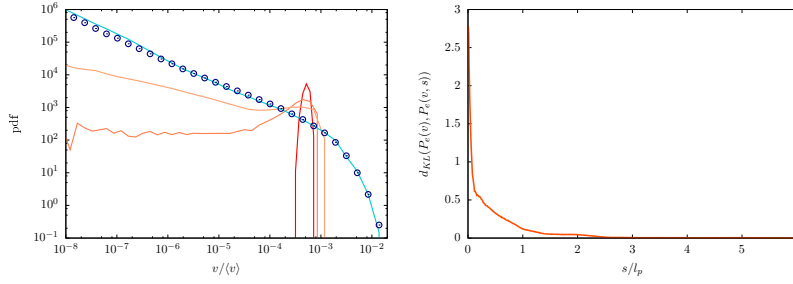


Fig. 3 (Left) The Eulerian velocity PDF computed on cubes centered in the middle of the sample of sizes $V = 4 \cdot 10^{-8}V_T$ (red solid line), $V = 1 \cdot 10^{-6}V_T$ (dark orange solid line), $V = 10^{-5}V_T$ (light orange solid line), $V = 1.25 \cdot 10^{-1}V_T$ (light blue solid line) and V_T (navy blue circles), where V_T is the bulk volume of the sample. (Right) The KL divergence between the full sample Eulerian velocity PDF and the Eulerian velocity PDFs computed on growing volumes from $V = 0$ to $V = V_T$.

256 First, we determine the porosity REV. Figure 1 displays the evolution of the ratio
 257 ϕ_ℓ between void and bulk volume computed on a size increasing domain that starts
 258 from a single point in the center of the sample to the total sample volume. The porosity
 259 starts from a value of one since the initial volume is situated in the void space.
 260 It then converges towards the porosity value of $\phi = 0.182$ after about $4.5\ell_p$, which
 261 means that the sample is an REV for porosity.

262 Second, we investigate the convergence of the Eulerian velocity statistics with in-
 263 creasing support scale. Figure 3a displays the Eulerian velocity PDFs respectively
 264 computed on cubes of volumes $V = 4 \cdot 10^{-8}V_T$, $V = 10^{-6}V_T$, $V = 10^{-5}V_T$, $V =$
 265 $1.25 \cdot 10^{-1}V_T$, and V_T , where V_T is the bulk volume of the sample. We observe that the
 266 distribution evolves toward the full sample distribution as the volume of the cube in-
 267 creases. For $V = 4 \cdot 10^{-8}V_T$ we measure a small range of velocities. For $V = 10^{-6}V_T$
 268 the distribution looks like the velocity distribution sampled in a single pore. The
 269 distribution sampled in a volume $V = 10^{-5}V_T$ corresponds to the average of several
 270 pore velocity distributions. Finally, the same statistics are observed for volumes
 271 $V = 1.25 \cdot 10^{-1}V_T$ and V_T , despite the former being 8 times smaller than the latter. To
 272 quantify accurately the convergence toward the Eulerian PDF, we use the aforemen-
 273 tioned KL divergence between the successive $p_\ell(v)$ and $p_e(v)$. The distance between
 274 the full sample velocity PDF and the subsequent growing cubes velocity PDFs is dis-
 275 played in Figure 3b. For small volumes V the KL divergence to the velocity PDF of
 276 the full sample is large since the volume only contains a restricted range of the veloc-
 277 ity spectrum. Then, the KL divergence decreases quickly as the evolving distribution
 278 approaches the reference distribution. A distance $d_{KL} < 10^{-2}$ is reached for a volume
 279 $V \approx 0.125V_T$. In other words, the limit distribution is attained. This indicates that the
 280 sample volume is noticeably larger than the Eulerian velocity REV.

281 We have seen that an REV for the Eulerian velocity magnitude exists. Now we
 282 investigate the stationarity of the velocity process by considering the evolution of
 283 $p_s(v, s)$ for a given initial velocity distribution $p_0(v)$ toward the steady state $p_s(v)$.
 284 To investigate accurately this evolution, we inject at the inlet particles in a given
 285 velocity range $v \in [v_l, v_u]$ and allocate the same weight to the whole range (see blue

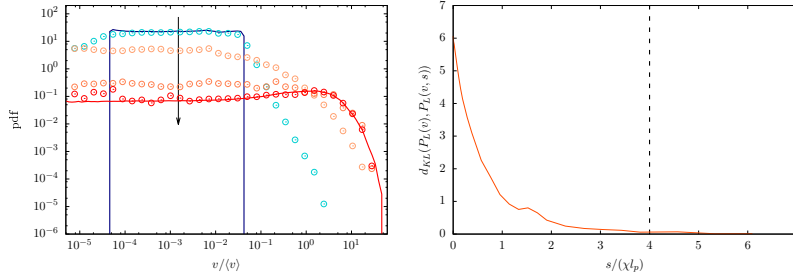


Fig. 4 (Left panel) The Lagrangian PDF $p_s(v, s)$ along an ensemble of streamlines measured at distance $s = \ell_p/15$ (light blue circles), $s = 4\ell_p/3$ (light orange circles), $s = 20\ell_p/3$ (dark orange circles) and $s = 32\ell_p/3$ (red circles). The blue solid line denotes the initial velocity PDF at $s = 0$ and the red solid line indicates the steady-state Lagrangian s-velocity PDF. (Right panel) The KL divergence (orange curve) between the steady-state Lagrangian velocity PDF and the successive Lagrangian velocity PDFs computed at increasing distances from $s = 0$ to $s = 10\ell_p$.

286 solid curve in the right panel of Figure 4). The resulting distribution is far from the
 287 steady-state distribution. We display the evolution of this distribution with distance
 288 in Figure 4a. The distribution converges toward the steady-state $p_s(v)$ after a distance
 289 of $s = 20\ell_p/3$.

290 As above we quantify convergence by computing the KL distance between the
 291 steady-state velocity PDF $p_s(v)$ and the distributions $p_s(v, s)$ computed after different
 292 distances s along the particle streamlines (see, also Puyguiraud et al, 2019a). The
 293 right panel of Figure 4 displays the evolution of the KL divergence with distance
 294 s along the streamline. At small distances the KL-divergence between $p_s(v, s)$ and
 295 the steady state $p_s(v)$ is large because the initial distribution is very different from
 296 the steady state distribution. The KL-divergence then decreases with increasing s ,
 297 and reaches the threshold $\varepsilon = 5 \cdot 10^{-2}$ after $s = 20\ell_p/3$, which corresponds to an
 298 average linear distance of $4\ell_p$. Despite the fluctuations that we observe in $p_s(v, s)$ at
 299 distances $s \geq 20\ell_p/3$, we consider the convergence to be satisfactory because the KL
 300 divergence remains below ε . The small fluctuations are due to the complexity of the
 301 geometry that particles encounter. In conclusion the sample fulfills the stationarity
 302 conditions required for the upscaling.

303 3 Implications for Darcy Scale Transport

304 We have seen in the previous section that both Fickian transport descriptions in terms
 305 of Brownian dynamics as well as anomalous transport theories based on continuous
 306 time random walks require the existence of an REV in terms of the Eulerian velocity
 307 distribution. This is a necessary condition for the particle velocity series to be station-
 308 ary and ergodic. Furthermore, we have seen that transport descriptions in terms of
 309 Brownian dynamics are valid at time scales that are much larger than the characteris-
 310 tic velocity correlation time. Thus, such approaches are only of limited applicability
 311 for situations characterized by broad distributions of the velocity persistence times

312 which are typical of natural porous media that display intermittent velocity time se-
 313 ries. These features can be captured naturally by the CTRW approach. In this section
 314 we illustrate the CTRW approach to upscale pore-scale particle motion and discuss
 315 the implications for modeling hydrodynamic dispersion.

316 First, it is worth recalling that the previous sections focused on purely advective
 317 transport. This means, advective sampling of velocity contrast along streamlines is
 318 the only mechanism by which particles can experience the velocity heterogeneity
 319 and eventually become statistically equal, or in other words, for Lagrangian velocity
 320 statistics to become stationary and ergodic. In this sense, the purely advective case
 321 represents a worst case scenario because molecular diffusion is an additional sam-
 322 pling mechanism that makes particles experience the velocity contrast across stream-
 323 lines, as in the problem of Taylor dispersion in a pipe (Taylor, 1953). In fact, diffu-
 324 sion impacts on pore scale transport in various various ways. Diffusive smoothing
 325 reduces the velocity contrast between particles, sets a maximum transition time over
 326 the length of a pore, and can lead to trapping in cavities and dead end pores (Saffman,
 327 1959; Bijeljic and Blunt, 2006b; Dentz et al, 2018).

328 Thus, regarding the velocity sampling and the convergence toward stationarity,
 329 diffusion is favorable because it sets a maximum sampling time. Nevertheless, sim-
 330 ilarly to the purely advective case, a representative part of the velocity distribution
 331 needs to be available on the support scale. Thus, the presence of diffusion does not
 332 change the main conclusion regarding the existence and definition of the REV. Yet,
 333 it affects the stochastic particle dynamics because it introduces a temporal sampling
 334 mechanism in addition to the spatial sampling along streamlines. These aspects can
 335 be taken into account in the CTRW framework (Bijeljic and Blunt, 2006b; Dentz
 336 et al, 2018).

337 In the following, we briefly recall some basic relations of the CTRW. As described
 338 in Section 2.2.2, the CTRW models particle motion through the coupled space-time
 339 transitions (12). For purely advective particle motion, the transition time distribution
 340 $\psi(t)$ is given in terms of the stationary velocity distribution $p_s(v)$ as

$$341 \quad \psi(t) = \frac{\ell_c}{t^2} p_s(\ell_c/t). \quad (17)$$

343 The impact of diffusion on velocity sampling, the introduction of a maximum transi-
 344 tion time and trapping in cavities and low velocities zones can be modeled in terms
 345 of a coupled distribution $\psi(x,t)$ of transition lengths and times (Dentz et al, 2018,0).
 346 The evolution of the particle distribution $p(x,t)$ is given by the generalized master
 347 equation (Berkowitz et al, 2006)

$$348 \quad \frac{\partial p(x,t)}{\partial t} = \int_0^t dt' \mathcal{K}(x-x', t-t') [p(x', t') - p(x, t)], \quad (18)$$

350 where the memory kernel $\mathcal{K}(x,t)$ is defined through its Laplace transform by

$$351 \quad \hat{\mathcal{K}}(x, \lambda) = \frac{\lambda \hat{\psi}(x, \lambda)}{1 - \hat{\psi}(\lambda)}, \quad (19)$$

353 Note that this formulation implicitly assumes that the transition lengths and times
 354 are stationary, this means the joint distribution of transition lengths and times for the
 355 first step is equal to $\psi(x, t)$, which in general may not be case, depending on the
 356 injection condition (Dentz et al, 2016). We notice that $p(x, t)$ is the particle density in
 357 a unit bulk volume. Thus, it is related to the concentration $c(x, t)$ in the fluid phase as
 358 $p(x, t) = \phi c(x, t)$. We assume that $\psi(x, t)$ is sharply peaked around the characteristic
 359 length scale ℓ_c . Thus one can expand the integrand on the right side of (18) up to
 360 second order in the displacement increment to obtain (Berkowitz et al, 2006)

$$361 \quad \phi \frac{\partial c(x, t)}{\partial t} = - \int_0^t dt' \left[\mathcal{K}_v(t-t') \phi \frac{\partial c(x, t')}{\partial x} - \mathcal{K}_D(t-t') \phi \frac{\partial^2 c(x, t')}{\partial x^2} \right], \quad (20)$$

363 where we defined the advection and dispersion kernels in terms of their Laplace trans-
 364 forms as

$$365 \quad \hat{\mathcal{K}}_v = \int dx x \hat{\mathcal{K}}(x, \lambda), \quad \hat{\mathcal{K}}_D = \int dx x^2 \hat{\mathcal{K}}(x, \lambda). \quad (21)$$

367 Equations (18) and (20) describe in general non-Fickian transport (Berkowitz et al,
 368 2006). In the absence of trapping and for times larger than the characteristic diffusion
 369 time scale ℓ_c^2/D (with D the molecular diffusion coefficient), the non-local advection-
 370 dispersion equation localizes and gives the advection-dispersion model (3) (Dentz
 371 et al, 2004).

372 Note that, since the REV is defined in terms of the Eulerian statistics inside the
 373 domain, the diffusion process has no impact on the REV definition and therefore
 374 does not affect its size. However, it will affect the times scales to reach ergodic con-
 375 ditions. Indeed, in a purely advective case particles sample velocities as they move
 376 along streamlines. In the presence of diffusion, particles can sample velocities addi-
 377 tionally by changing streamlines, which may accelerate the convergence to a steady
 378 state distribution. Thus, defining the REV for purely advective transport guaranties
 379 its validity for any finite value of the Péclet number.

380 4 Conclusions

381 In this paper we aimed at answering the following question: Is there an REV for
 382 anomalous dispersion? We showed that an REV not only exists, but that its existence
 383 is also a necessary condition for CTRW approaches to non-Fickian hydrodynamic
 384 dispersion to be valid. The REV definition is set in terms of the Eulerian velocity
 385 statistics. Precisely, the REV scale is defined as the length scale of the sampling vol-
 386 ume beyond which the spatially sample velocity distribution remains invariant. This
 387 definition requires the sample to be also a porosity REV since an evolving porosity
 388 would prevent the convergence of the Eulerian velocity distribution. The existence
 389 of an REV is a necessary conditions for the upscaling of anomalous dispersion us-
 390 ing the CTRW approach. It requires the Lagrangian velocity series to form stationary
 391 stochastic processes that relaxes toward the stationary velocity distribution within a
 392 characteristic length scale. In other words, for a given sample a steady-state velocity

393 distribution needs to exist. In conclusion, if a sample fulfills these criteria, anomalous and as well as Fickian hydrodynamic dispersion can be upscaled by the CTRW
394 approach.
395

396 **Acknowledgements** The research leading to these results has received funding from the European Re-
397 search Council under the European Union's Seventh Framework Programme (FP7/2007-2013)/ ERC Grant
398 Agreement No. 617511 (MHetScale). This work was partially funded by the CNRS-PICS project CROSS-
399 CALE, project number 280090.

400 References

- 401 Bear J (1972) Dynamics of fluids in porous media. American Elsevier, New York
- 402 Berkowitz B, Cortis A, Dentz M, Scher H (2006) Modeling non-fickian transport in
403 geological formations as a continuous time random walk. *Reviews of Geophysics*
404 44(2)
- 405 Bigi B (2003) Using kullback-leibler distance for text categorization. In: European
406 Conference on Information Retrieval, Springer, pp 305–319
- 407 Bijeljic B, Blunt MJ (2006a) Pore-scale modeling and continuous time
408 random walk analysis of dispersion in porous media. *Water Resources*
409 *Research* 42(1), 10.1029/2005WR004578, URL [https://agupubs](https://agupubs.onlinelibrary.wiley.com/doi/abs/10.1029/2005WR004578)
410 [.onlinelibrary.wiley.com/doi/abs/10.1029/2005WR004578](https://agupubs.onlinelibrary.wiley.com/doi/pdf/10.1029/2005WR004578), [https://](https://agupubs.onlinelibrary.wiley.com/doi/pdf/10.1029/2005WR004578)
411 agupubs.onlinelibrary.wiley.com/doi/pdf/10.1029/2005WR004578
- 412 Bijeljic B, Blunt MJ (2006b) Pore-scale modeling and continuous time random walk
413 analysis of dispersion in porous media. *Water resources research* 42(1)
- 414 Bijeljic B, Mostaghimi P, Blunt MJ (2011) Signature of non-fickian solute transport
415 in complex heterogeneous porous media. *Phys Rev Lett* 107(20):204,502
- 416 Cortis A, Berkowitz B (2004) Anomalous transport in “classical” soil and sand
417 columns. *Soil Science Society of America Journal* 68(5):1539, 10.2136/sssaj2004
418 .1539, URL <https://doi.org/10.2136/sssaj2004.1539>
- 419 Cushman JH, Moroni M (2001) Statistical mechanics with three-dimensional particle
420 tracking velocimetry experiments in the study of anomalous dispersion. i. theory.
421 *Physics of Fluids* 13(1):75–80, 10.1063/1.1328075, URL [https://doi.org/10](https://doi.org/10.1063/1.1328075)
422 [.1063/1.1328075](https://doi.org/10.1063/1.1328075)
- 423 De Anna P, Le Borgne T, Dentz M, Tartakovsky AM, Bolster D, Davy P (2013) Flow
424 intermittency, dispersion, and correlated continuous time random walks in porous
425 media. *Physical review letters* 110(18):184,502
- 426 De Anna P, Quaipe B, Biroš G, Juanes R (2017) Prediction of velocity distribution
427 from pore structure in simple porous media. *Phys Rev Fluids* 2:124,103, 10.1103/
428 [PhysRevFluids.2.124103](https://doi.org/10.1103/PhysRevFluids.2.124103)
- 429 Dentz M, Cortis A, Scher H, Berkowitz B (2004) Time behavior of solute transport in
430 heterogeneous media: transition from anomalous to normal transport. *Adv Water*
431 *Resour* 27(2):155–173
- 432 Dentz M, Kang PK, Comolli A, Le Borgne T, Lester DR (2016) Continuous time
433 random walks for the evolution of lagrangian velocities. *Physical Review Fluids*
434 1(7):074,004

- 435 Dentz M, Icardi M, Hidalgo JJ (2018) Mechanisms of dispersion in a porous medium.
436 *Journal of Fluid Mechanics* 841:851–882, 10.1017/jfm.2018.120, URL <https://doi.org/10.1017/jfm.2018.120>
437
- 438 Gardiner C (2010) *Stochastic Methods*. Springer Verlag Berlin-Heidelberg
- 439 Holzner M, Morales VL, Willmann M, Dentz M (2015) Intermittent lagrangian ve-
440 locities and accelerations in three-dimensional porous medium flow. *Phys Rev E*
441 92:013,015
- 442 Kang PK, de Anna P, Nunes JP, Bijeljic B, Blunt MJ, Juanes R (2014) Pore-
443 scale intermittent velocity structure underpinning anomalous transport through
444 3-d porous media. *Geophysical Research Letters* 41(17):6184–6190, 10.1002/
445 2014GL061475, URL <http://dx.doi.org/10.1002/2014GL061475>
- 446 Koponen A, Kataja M, Timonen J (1996) Tortuous flow in porous media. *Physical*
447 *Review E* 54(1):406
- 448 Kullback S, Leibler RA (1951) On information and sufficiency. *The annals of math-*
449 *ematical statistics* 22(1):79–86
- 450 Lindgren B, Johansson AV, Tsuji Y (2004) Universality of probability density distri-
451 butions in the overlap region in high reynolds number turbulent boundary layers.
452 *Physics of fluids* 16(7):2587–2591
- 453 Liu Y, Kitanidis PK (2012) Applicability of the Dual-Domain Model to Nonaggre-
454 gated Porous Media. *Ground Water* 50(6):927–934
- 455 Meyer DW, Bijeljic B (2016) Pore-scale dispersion: Bridging the gap between micro-
456 scopic pore structure and the emerging macroscopic transport behavior. *Physical*
457 *Review E* 94(1):013,107
- 458 Morales VL, Dentz M, Willmann M, Holzner M (2017) Stochastic dynamics of inter-
459 mittent pore-scale particle motion in three-dimensional porous media: Experiments
460 and theory. *Geophysical Research Letters* 44(18):9361–9371
- 461 Moroni M, Cushman JH (2001) Statistical mechanics with three-dimensional par-
462 ticle tracking velocimetry experiments in the study of anomalous dispersion. II.
463 experiments. *Physics of Fluids* 13(1):81–91, 10.1063/1.1328076, URL <https://doi.org/10.1063/1.1328076>
464
- 465 Noetinger B, Roubinet D, Russian A, Le Borgne T, Delay F, Dentz M, De Dreuzy
466 JR, Gouze P (2016) Random walk methods for modeling hydrodynamic transport
467 in porous and fractured media from pore to reservoir scale. *Transport in Porous*
468 *Media* pp 1–41
- 469 Painter S, Cvetkovic V (2005) Upscaling discrete fracture network simulations:
470 An alternative to continuum transport models. *Water Resour Res* 41:W02,002,
471 10.1029/2004WR003682
- 472 Puyguiraud A, Gouze P, Dentz M (2019a) Stochastic dynamics of lagrangian
473 pore-scale velocities in three-dimensional porous media. *Water Resources*
474 *Research* 55, 10.1029/2018WR023702, [https://agupubs.onlinelibrary](https://agupubs.onlinelibrary.wiley.com/doi/pdf/10.1029/2018WR023702)
475 [.wiley.com/doi/pdf/10.1029/2018WR023702](https://agupubs.onlinelibrary.wiley.com/doi/pdf/10.1029/2018WR023702)
- 476 Puyguiraud A, Gouze P, Dentz M (2019b) Upscaling of anomalous pore-scale dis-
477 persion. *Transport in Porous Media*
- 478 Robert R, Sommeria J (1991) Statistical equilibrium states for two-dimensional
479 flows. *Journal of Fluid Mechanics* 229:291–310, 10.1017/S0022112091003038

-
- 480 Saffman P (1959) A theory of dispersion in a porous medium. *Journal of Fluid Me-*
481 *chanics* 6(03):321–349
- 482 Taylor G (1953) Dispersion of soluble matter in solvent flowing slowly through a
483 tube. *Proceedings of the Royal Society of London Series A, Mathematical and*
484 *Physical Sciences* 219(1137):186–203, URL [http://www.jstor.org/stable/](http://www.jstor.org/stable/99386)
485 99386